Equilibria in Solutions of Nucleosides, 5′-Nucleotides, and dienPd^{2+} [1]

Kurt H. Scheller, Verena Scheller-Krattiger, and R. Bruce Martin*

Contribution from the Chemistry Department, University of Virginia, Charlottesville, Virginia 22901. *Received May 11, 1981*

Abstract: A comprehensive analysis of the binding of the diethylenetriamine chelate of tetragonal Pd(II) to pyrimidine and purine nucleosides and purine 5′-monophosphates has been performed by proton magnetic resonance spectroscopy. Equilibria are readily achieved with Pd(II), and the results serve as a reference for slowly reacting Pt(II). Stability constants are presented for dienPd^{2+} binding to N(3) of cytidine, uridine, and thymidine, and to N(1) and N(7) of inosine, 5′-IMP, 5′-GMP, adenosine, and 5′-AMP. The dichotomy of N(1) vs. N(7) binding is resolved by comparison of intensities in proton magnetic resonance spectra. Chemical shifts of all free-ligand and mononuclear and binuclear complexes are assigned over the $1 < pH < 12$ range. Ligand distribution curves for approximately equimolar 0.1 M mixtures of dienPd^{2+} and ligand are presented over the same pH region. Though the basicity of N(1) is much greater than that of N(7) in purines, dienPd^{2+} only slightly favors N(1). By designating nucleoside or its 5′-phosphate by its first letter and the nitrogen binding site by its ring position, the order of decreasing stability constants for dienPd^{2+} binding is T3 > U3 > I1 > G7 > G1 > I7 ≫ C3 > A1 > A7. Because of the proton at N(3) in the pyrimidines and at N(1) in the 6-oxopurines the order of stabilities is pH dependent. At pH 7 the stability order for dienPd^{2+} becomes G7 > I7 > I1 > G1 > U3 > T3 > C3 > A1 > A7. Binding of dienPd^{2+} at N(7) promotes the phosphate deprotonation and, by up to 2 log units, the N(1) deprotonation.

Despite numerous studies on the binding of metal ions to the nucleic bases of nucleosides and nucleotides, reliable stability constants remain scarce.[2] With their dichotomy of binding at N(1) and N(7) the purine derivatives pose a special problem. The weakly basic N(7) site, which is not protonated until pH <3, often binds metal ions with a stability comparable to that of the more basic N(1) site. Since this N(1)–N(7) dichotomy is difficult to resolve by potentiometric titrations, other physical techniques are required.

^{1}H nuclear magnetic resonance spectroscopy will determine separate metal ion stabilities at N(1) and N(7) if two conditions are met. The metal ion should be diamagnetic so that broadening and extreme shifting of NMR peaks do not occur. In addition the metal ion should be in slow exchange between coordination sites so that the population of each individual complex may be measured. From several studies it is evident that Pd(II) meets the two conditions.[3-5] Furthermore, the comparable stereochemistry of Pd(II) and Pt(II) makes Pd(II) compounds excellent vehicles for the study of the anticipated thermodynamic properties of Pt(II) complexes, many of which are effective antitumor agents.[6] Reactions of Pt(II) occur slowly, however, and from comparison with related Pd(II) complexes it has been argued that reported constants of the ethylenediamine (en) complex of Pt(II) with nucleosides are grossly underestimated.[7]

In this research we report the absolute values of stability constants for binding of the diethylenetriamine (dien) complex of tetragonal Pd(II) with all five common nucleic bases and hypoxanthine in their nucleoside and/or nucleoside monophosphate forms. With only a single site available for substitution, dienPd$(H_2O)^{2+}$ avoids complexities offered by enPd$(H_2O)_2^{2+}$ [8] and provides an intrinsic measure of Pd(II) binding at individual nucleic base sites.

Experimental Section

Nucleosides and 5′-nucleotides were of the highest grade available from Sigma Chemical Co. Stock solutions of dienPd$(H_2O)^{2+}$ at 0.1 M were prepared by suspending [dienPdI]I in D_2O, adding 1.98 equiv of $AgNO_3$, and stirring overnight. The precipitate was filtered and the resulting yellow solution used directly. Proton NMR spectra were recorded on a Varian EM 390 (90 MHz) spectrometer at 34 °C and a sweep width of 2 ppm. A frequency counter was used for accurate determination of chemical shifts. Most experiments were performed at 0.10 M dienPd^{2+} and 0.10 to 0.14 M ligand. For competition experiments the solutions were in addition 0.1 M in uridine or cytidine. The pK_a values for the uncoordinated ligands were obtained by titrating the ligands in the absence of dienPd^{2+}. These solutions were 25 mM in ligand, except for adenosine which was 5 mM. Addition of a trace of EGTA to remove paramagnetic impurities resulted in marked sharpening of NMR peaks. Standing for at least 20 min and constancy of pH before and after NMR spectra were taken assured attainment of equilibrium. The titration curves were calculated with a nonlinear least-squares program that fitted chemical shift to pH by theoretical equations. *tert*-Butyl alcohol served as an internal reference. However, all chemical shifts are reported downfield from DSS (2,2-dimethyl-2-silapentane-5-sulfonate) by adding 1.234 ppm to the recorded *tert*-butyl alcohol referenced shifts. High concentrations of aromatic compounds may cause some shift displacement of the internal reference *tert*-butyl alcohol.[9] The reliability of *tert*-butyl alcohol as internal reference was checked in two ways. The chemical shift difference between internal *tert*-butyl alcohol and internal tetramethylammonium ion, a stable reference,[10] was found to increase by ≤0.008 ppm, a difference too small to influence any conclusions in this paper. In several cases pK_a values were calculated by using the shift

Table I. Limiting Chemical Shifts and pK_a Values for GMP and Its dienPd^{2+} Complexes

species	phosphate	pK_a[a]	H(8) shift[b]
$^+H_2BH_1H_P$	−1	2.37	9.053
BH_1H_P	−1	6.23	8.081
BH_1	−2	9.73	8.187
B^-	−2		8.105
$M_2BH_1H_P$	−1	5.84	8.441
M_2BH_1	−2	8.67	8.697
M_2B^-	−2		8.552
$M_2BM_1H_P$	−1	5.91	8.308
M_2BM_1	−2		8.578
BM_1	−2		8.097

[a] ±0.03. [b] Usually ±0.005 or better.

(1) This research was supported by grants from the National Cancer Institute (CA-14832) and from the National Science Foundation.
(2) Martin, R. B.; Mariam, Y. H. *Met. Ions Biol. Syst.* **1979**, *8*, 57.
(3) Nelson, D. J.; Yeagle, P. L.; Miller, T. L.; Martin, R. B. *Bioinorg. Chem.* **1976**, *5*, 353.
(4) Lim, M. C.; Martin, R. B. *J. Inorg. Nucl. Chem.* **1976**, *38*, 1915.
(5) Vestues, P. I.; Martin, R. B *Inorg. Chim. Acta* **1981**, *55*, 99.
(6) Sigel, H., Ed. "Metal Ions in Biological *Systems*"; Marcel Dekker, New York, 1980; Vol. 10 and 11.
(7) Vestues, P. I.; Martin, R. B. *J. Am. Chem. Soc.* **1981**, *103*, 806.
(8) Sovago, I.; Martin, R. B. *Inorg. Chem.* **1980**, *19*, 2868.
(9) Jones, R. A. Y.; Katritzky, A. R.; Murell, J. N.; Sheppard, N. *J. Chem. Soc.* **1962**, 2576.
(10) Scheller, K. H.; Hofstetter, F.; Mitchell, P. R.; Prijs, B.; Sigel, H. *J. Am. Chem. Soc.* **1981**, *103*, 247.

0002-7863/81/1503-6833$01.25/0

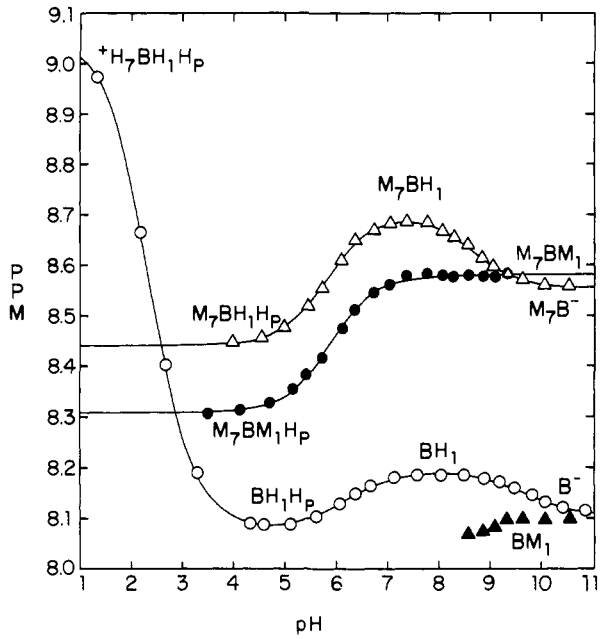

Figure 1. 5′-GMP H(8) chemical shift vs. pH for several species. Open circles refer to free ligand, open triangles to complex with dienPd^{2+} at N(7), closed triangles to complex with dienPd^{2+} at N(1), and closed circles to binuclear complex with dienPd^{2+} at both N(1) and N(7). The ppm scale is downfield from DSS.

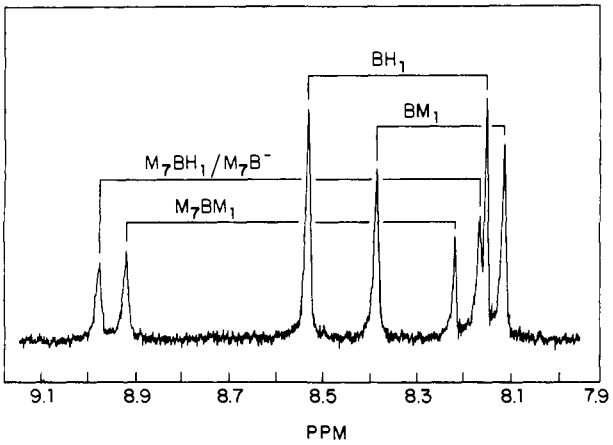

Figure 2. ^{1}H NMR spectrum of 0.12 M 5′-IMP and 0.1 M dienPd^{2+} in D_2O at pH 7.8. H(2) signals occur upfield and H(8) signals downfield of 8.3 ppm.

difference between H(8) and H(2). The results agreed within experimental error with those calculated with the *tert*-butyl alcohol referenced shifts. Peaks due to H(8) in ligands containing either hypoxanthine or adenine as base were assigned by exchange with solvent deuterium. All results in this paper were obtained in greater than 98% D_2O solvent. The ionic strength was about 0.5, controlled with KNO_3. The pH values are not corrected for D_2O.[11]

Results

Species Characteristics. H(8) chemical shifts downfield from DSS for GMP and its complexes with dienPd^{2+} as a function of pH are shown in Figure 1. The limiting chemical shifts for each speecies and its pK_a value derived from a nonlinear least-squares fit of chemical shift vs. pH are tabulated in Table I. Subscripts

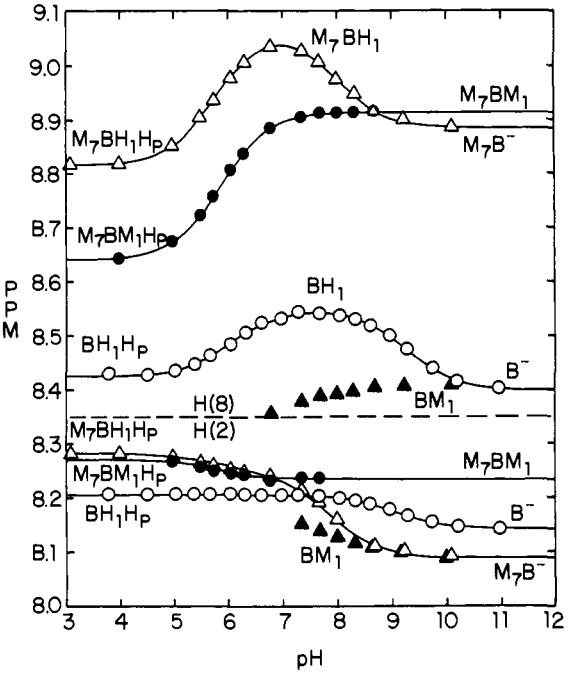

Figure 3. 5′-IMP H(8) and H(2) chemical shift vs. pH for several species. All points downfield of 8.3 ppm are H(8) shifts and all points upfield of 8.3 ppm are H(2) shifts. Symbols are the same as in the Figure 1 caption.

Table II. Limiting Chemical Shifts and pK_a Values for IMP, Inosine, and Their dienPd^{2+} Complexes

species	phosphate	pK_a[a]	chemical shift[b] H(8)	chemical shift[b] H(2)
$^+H_2BH_1H_P$	−1	1.3	9.30	8.40
BH_1H_P	−1	6.00	8.422	8.205
BH_1	−2	9.27	8.545	8.204
B^-	−2		8.397	8.142
$M_7BH_1H_P$	−1	5.76	8.815	8.281
M_7BH_1	−2	8.00	9.064	8.248
M_7B^-	−2		8.885	8.089
$M_7BM_1H_P$	−1	5.87	8.640	8.268
M_7BM_1	−2		8.913	8.234
BM_1	−2		8.41	8.09
BH_1	*c*	9.06	8.311	8.206
B^-	*c*		8.122	8.120
M_7BH_1	*c*	7.60	8.680	*d*
M_7B^-	*c*		8.417	*d*
M_7BM_1	*c*		8.485	8.261
BM_1	*c*		8.13	8.13

[a] ±0.03 except for $^+H_7BH_1H_P$ which is ±0.1. [b] Usually ±0.005 or better. [c] Inosine. [d] Peaks intermingled.

1 and 7 on H or M designate a proton or dienPd^{2+} at N(1) and N(7) nitrogens, respectively, of the purine ring. The downfield H(8) chemical shifts upon increasing the pH from 5 to 7.5 result from phosphate deprotonation, $RPO_3H^- \rightarrow RPO_3^{2-}$. An H_p in the tables and figures designates a protonated RPO_3H^- group. The upfield chemical shifts from pH 7.5 to 11 are due to ionization at uncomplexed N(1) in the free ligand BH_1 and N(7) complexed M_7BH_1 species. In the most acidic solutions protonation at N(7) of the free ligand with a neutral purine ring to give $^+H_7BH_1H_P$ in GMP produces a large downfield shift of 0.98 ppm and occurs with a pK_a = 2.37 ± 0.02. The curve for the free GMP shown in Figure 1 was titrated in the absence of dienPd^{2+} at 25 mM. However, limiting shifts and pK_a values approach those evaluated from solutions containing dienPd^{2+}.

Figure 2 depicts a representative ^{1}H NMR spectrum of H(8) and H(2) for IMP and its dienPd^{2+} complexes at pH 7.8. Figure

(11) It is usual to define $pH_D = pH_{obsd} + 0.40$. pK_a values obtained in D_2O are approximately related to those in H_2O by the equation pK_D = 1.015(pK_H) + 0.45, plus a possible term for charge effects.[12] Since the constant terms in the two equations nearly cancel each other for many molecules, the observed pK_a in D_2O resembles that determined in water.

(12) Martin, R. B. *Science* **1963**, *139*, 1198.
(13) Lim, M. C. *J. Inorg. Nucl. Chem.* **1981**, *43*, 221.
(14) Lim, M. C.; Martin, R. B. *J. Inorg. Nucl. Chem.* **1976**, *38*, 1911.

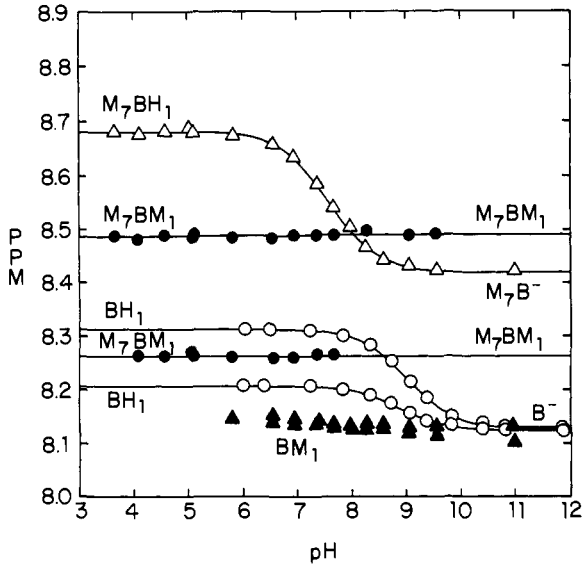

Figure 4. Inosine H(8) and H(2) chemical shift vs. pH. For the same species the H(8) shifts are always at lower field than H(2) shifts, except for BM_1 where the assignment is uncertain. Symbols are the same as in Figure 1 caption.

Table III. Limiting Chemical Shifts and pK_a Values for AMP, Adenosine, and Their dienPd^{2+} Complexes

species	phosphate	pK_a[a]	chemical shift[b] H(8)	H(2)
$^+BH_1H_P$	−1	4.05	8.617	8.445
BH_P	−1	6.23	8.421	8.185
B	−2		8.559	8.210
$M_7BH_1^+H_P$	−1	2.3	9.24	8.49
M_7BH_P	−1	5.70	8.987	8.280
M_7B	−2		9.254	8.247
BM_1H_P	−1	6.10	8.449	8.611
BM_1	−2		8.588	8.584
$M_7BM_1H_P$	−1	5.67	9.070	8.750
M_7BM_1	−2		9.332	8.724
BH_1^+	*c*	3.89	8.536	8.453
B	*c*		8.315	8.235
$M_7BH_1^+$	*c*	2.0	9.16	8.55
M_7B	*c*		8.884	8.309
BM_1	*c*		8.37	8.622
M_7BM_1	*c*		8.988	8.760

[a] ±0.03, except for $M_7BH_1^+$ and $M_7BH_1^+H_P$ which are ±0.1. [b] ±0.003, except for $M_7BH_1^+$ and $M_7BH_1^+H_P$ which are ±0.01. [c] Adenosine.

3 shows the pH dependence of both H(8) and H(2) chemical shifts for each species in the IMP system. H(8) shifts occur downfield of 8.3 ppm and H(2) shifts occur upfield. Table II lists the limiting shifts for each species and pK_a values derived from the H(8) shifts. For H(2) the shift range is smaller and the margin of error greater, but derived pK_a values were similar. As for GMP, protonation at N(7) of free IMP with a neutral purine ring gives rise to a large downfield H(8) shift of 0.88 ppm but occurs in more acidic solution with pK_a = 1.3.

Figure 4 shows the pH dependence of H(8) and H(2) chemical shifts of inosine and its dienPd^{2+} complexes. The corresponding limiting chemical shifts appear at the end of Table II. For inosine and IMP the chemical shift of H(8) on deprotonation at N(1) exceeds the shift of the nearer H(2). The curves for free IMP and inosine in Figures 3 and 4, respectively, were obtained by titrating these ligands at 25 mM in the absence of dienPd^{2+}. In the presence of dienPd^{2+} several complex and free-ligand species exhibit similar chemical shifts.

AMP and adenosine H(8) and H(2) chemical shifts as a function of pH appear in Figures 5 and 6, respectively. In contrast to IMP and inosine, the N(1) deprotonation of the free ligand yields a greater H(2) than H(8) shift. The limiting shifts for each

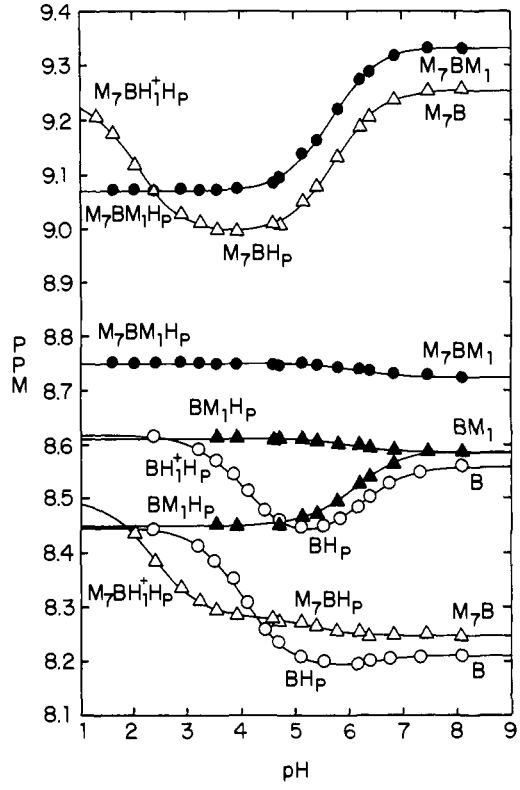

Figure 5. 5′-AMP H(8) and H(2) chemical shift vs. pH. Except for BM_1H_P, for the same species the H(8) shifts are always at lower field than the H(2) shifts. Symbols are the same as in the Figure 1 caption.

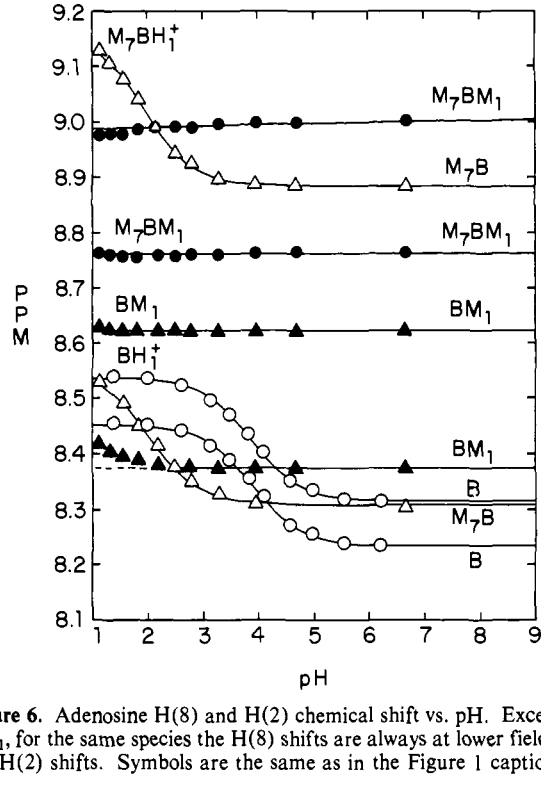

Figure 6. Adenosine H(8) and H(2) chemical shift vs. pH. Except for BM_1, for the same species the H(8) shifts are always at lower field than the H(2) shifts. Symbols are the same as in the Figure 1 caption.

free-ligand and dienPd^{2+} complex appear in Table III with the pK_a values derived from a nonlinear least-squares fit of observed chemical shift vs. pH. The free ligand shifts appearing in Figures 5 and 6 and Table III refer to solutions without dienPd^{2+}. In order to avoid excessive stacking only 5 mM adenosine was used, whereas AMP and all other ligands were 25 mM. Calculations with published stacking constants in neutral solutions show that under our conditions, for all ligands more than 87% are present in their

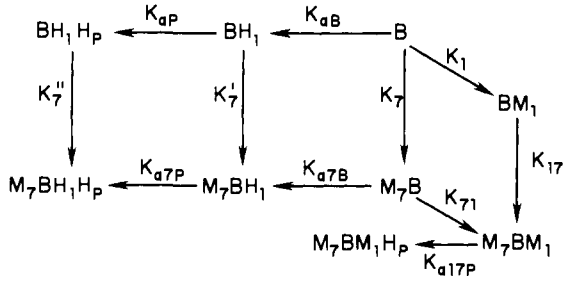

Figure 7. Equilibria in GMP and IMP complexes. Horizontal arrows refer to protonation, while vertical and diagonal arrows indicate coordination of metal ion. Numeral subscripts indicate site on nucleic base, N(1) and N(7). Subscript P designates a phosphate protonation. For inosine and adenosine the two furthest left species and $M_7BM_1H_P$ do not occur. For AMP phosphate protonation occurs at higher pH than base protonation, and instead of BH_1 and M_7BH_1 the species are BH_P and M_7BH_P.

unstacked monomeric form.[10] For solutions containing both 0.1 M adenosine and dienPd^{2+} the free-ligand peaks for H(8) and H(2) shift upfield 0.02 and 0.08 ppm, respectively. These upfield shifts are probably due to stacking interactions. Though there are hints of similar behavior with the other purine ligands, it is less extensive than for adenosine, as might be expected from their lower stacking tendency.[10]

The M_7BH_1 and M_7BM_1 complexes of GMP and IMP show a significant ionic strength dependency of the H(8) chemical shift. In the absence of added salt, a 20 mM solution of complex gave H(8) chemical shifts up to 0.1 ppm downfield of the same complex concentration in the presence of 0.75 M $NaClO_4$. Substitution of $NaNO_3$ did not alter the results. The ionic strength effect is almost complex charge independent over the range $4 < pH < 9$. The H(2) shift in the complexes and both the H(8) and H(2) shifts in unbound ligand are unaffected by a change in ionic strength.

Ligand Distribution. Identification of the chemical shifts assigned to free ligand and ligand bound to dienPd^{2+} in each complex over the entire pH range as shown in Figures 1 and 3–6 provides a firm basis for determination of stability constants and ligand distribution as a function of pH. Figure 7 shows equilibria among the several species that occur with GMP and IMP ligands. On the horizontal arrows in Figure 7 appear the pK_a values for both purine base and phosphate deprotonations. They are known from the pH dependence of the chemical shifts and the values are tabulated in Tables I and II. But the stability constants for dienPd^{2+} binding defined as indicated on vertical and diagonal arrows in Figure 7 remain to be evaluated. The research described so far allows some relative species distributions and ratios of stability constants to be set, but the absolute value for a stability constant must still be determined. Checks were made on the entire Figure 7 scheme for each ligand by a number of methods, some of which will be described below. The dichotomy of N(7) and N(1) in the purine bases and their complete complex formation with dienPd^{2+} at NMR concentrations prevent direct determination of stability constants. However, competition for binding to dienPd^{2+} between a purine base and another ligand with a known stability constant provides a chance to determine the desired binding constants. Pyrimidine nucleosides with only a single binding site at N(3) provide suitable ligands.

Stability constants of dienPd^{2+} to pyrimidine nucleosides were determined by competition with the proton for binding at the N(3) site. The stability constant may be calculated from the relative peak areas of bound and unbound ligand and knowledge of the pK_a. The pK_a values for protonation at N(3) were derived by the H(6) chemical shift dependence of the pH. Identical results were obtained from H(5) chemical shifts of cytidine and uridine. For cytidine with pK_a = 4.62 the stability constant log K_3 = 5.37 ± 0.04 was evaluated from solutions about 0.1 M in both total ligand and dienPd^{2+} at three different pH values between 1 and 1.5. A similar procedure was used for uridine at several pH values from 1.8 to 2.7 and for thymidine from pH 2.3–3.2 to obtain log K_3 values of 8.60 ± 0.05 and 8.67 ± 0.05, respectively. The results,

Table IV. Pyrimidine Nucleoside, Acidity and Stability Constants, and H(6) Chemical Shifts

			H(6) chemical shift		
nucleoside	pK_a	log K_3[b]	BH_3	B	dienPd^{2+}[c]
cytidine	4.62	5.37	8.109	7.806	7.868
uridine	9.53	8.60	7.837	7.650	7.646
thymidine	9.88	8.67	7.621	7.460	7.446

[a] ±0.02. [b] ±0.05. [c] No changes of coupling constants occur upon coordination.

recorded in Table IV, agree well with those found in a potentiometric study in H_2O.[13] The similar log K_3 values for uridine and thymidine indicate a negligible role for the 2′-hydroxy group of the uridine ribose, which is absent in the 2′-deoxyribose of thymidine.

In order to obtain an accurate ligand distribution over the entire pH range it is necessary to evaluate the pK_a for deprotonation of the bound water in dienPd$(H_2O)^{2+}$. Though the midpoint of the titration curve occurs near pH 7.5, the curve is too spread out on the pH axis to represent a simple ionization.[14] By assuming occurrence of a hydroxy-bridged complex we are able to obtain a good fit of the entire titration curve. The acidity constant for

$$2\text{dienPd}(H_2O)^{2+} \overset{K_1}{\rightleftharpoons} \text{dienPd–OH–Pd(dien)}^{3+} + H^+$$

$$\text{dienPd–OH–Pd(dien)}^{3+} \overset{K_2}{\rightleftharpoons} 2\text{dienPd(OH)}^{+} + H^+$$

the sum of the two reactions is given by $K_a = (K_1K_2)^{1/2}$. From a nonlinear least-squares fit of titration curves at 5 and 20 mM dienPd^{2+} and 0.5 M ionic strength (KNO_3) the results are pK_a = 7.74 ± 0.01 and log K_1 = −5.62 ± 0.04. The concentration of the hydroxy-bridged species reaches a maximum half-way through the titration, where pH = pK_a; e.g., in a 5 mM solution of dienPd^{2+} the maximum concentration of the hydroxy-bridged dimer is 0.57 mM. In the presence of other ligands such as nucleosides or nucleotides, the concentration of dimer is never significant. It is important, however, to consider the occurrence of dienPd(OH)$^+$ at pH >9. At this pH OH^- begins to displace adenosine and AMP from the fourth tetragonal position about dienPd^{2+}.

By comparing peak areas in ^{1}H NMR spectra competition for dienPd^{2+} between GMP and uridine was evaluated at pH 7.8 and 9.3. Consideration of all the GMP and uridine species, the previously derived pK_a values for GMP and uridine, and the stability constant for dienPd^{2+} binding to uridine lead for GMP to log K_1 = 7.86 ± 0.1 and log K_7' = 7.03 ± 0.1. The latter constant, in combination with the known pK_a values on the horizontal arrows in Figure 7 and the properties of a cyclic system, permit evaluation of log K_7 and log K_7''. These values are listed in Table V. Stability constant values may be checked by comparing the ratio of K_7/K_1 = 1.7, which is also given by the ratio of M_7B^- to BM_1. From two NMR spectra at pH 8.8 and 9.1 and the known pK_a value of M_7BH_1 a ratio of M_7B^- to BM_1 = 1.85 was calculated, in excellent agreement (to within 0.04 log units) with the value of 1.7. Concentration ratios of binuclear M_7BM_1 to mononuclear complexes and the properties of the cycle in Figure 7 that lead to M_7BM_1 allow calculation of log K_{17} and log K_{71}.

The collection of values in Table V for each ligand permits evaluation of the ligand distribution curve over the entire pH range for a given ratio of total dienPd^{2+} to total ligand concentration. For calculation of the distribution, the mass balance equations for Pd(II) and ligand, the electroneutrality equation, and the equilibrium constants for all species as indicated in Figure 7 were considered. Because an analytical solution to a system with so many equilibria becomes complex, an iterative approach was used and solved by computer. No approximations were made: all the resulting species distribution curves are exact solutions with the equilibrium constants given in Table V. A ligand distribution curve of ligand mole fraction (LMF) vs. pH for dienPd^{2+} binding to GMP is shown in Figure 8. The continuous curves derived from the equilibrium constants given in Table V agree well with the

Table V. Protonation (K_a) and Stability Constants (Logarithms) in Solutions Containing dienPd^{2+}

	inosine	IMP	GMP	adenosine	AMP
K_{aP}		6.00	6.23		6.23
K_{aB}	9.06	9.27	9.73	3.89	4.05
K_{a7P}		5.76	5.84		5.70
K_{a7B}	7.60	8.00	8.67	2.0	2.3
K_{a1P}					6.10
K_{a71P}		5.87	5.91		5.67
K_7''		6.14	6.64		2.76
K_7'	5.34	6.38	7.03	1.8	4.51
K_7	6.80	7.65	8.09	3.9	5.04
K_1	8.33	8.45	7.86	4.5	5.00
K_{71}	7.3	7.8	7.7	3.5	4.2
K_{17}	5.8	7.0	7.9	2.9	4.2
K_1'					4.87

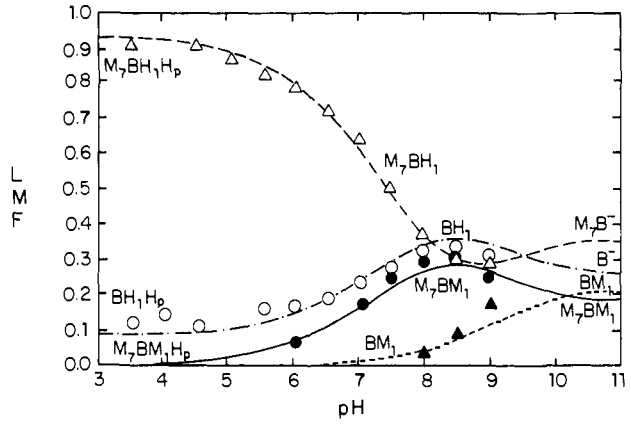

Figure 8. Species distribution of GMP binding by dienPd^{2+} presented as ligand mole fraction (LMF) vs. pH at 0.10 M dienPd^{2+} and 0.11 GMP. Curves derived from the equilibrium constants given in Table V correspond well to the individual points calculated from NMR intensities. Symbols are the same as in the Figure 1 caption.

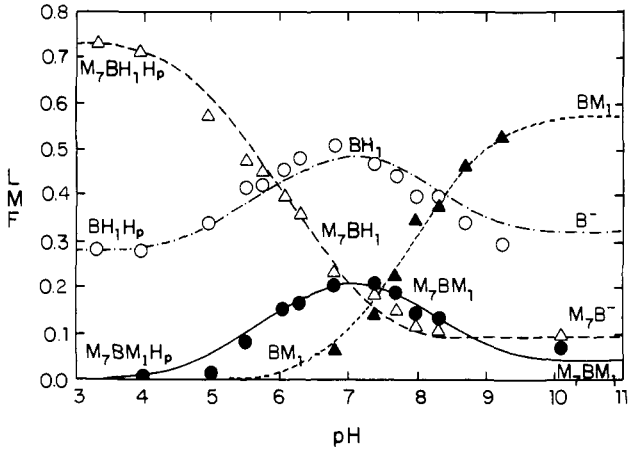

Figure 9. Species distribution of IMP binding by dienPd^{2+} presented as ligand mole fraction (LMF) vs. pH at 0.10 M dienPd^{2+} and 0.14 IMP. Curves derived from equilibrium constants in Table V compare favorably to the experimental points. Symbols are the same as in the Figure 1 caption.

experimental points. Even small changes in stability constants affect placement of the species distribution curves on the ligand mole fraction axis.

Species distribution curves for IMP and inosine derived by methods just described appear in Figures 9 and 10, respectively. The relatively large amounts of unbound ligand in these two figures result from the low ratios (0.72 and 0.77) of total dienPd^{2+} to total ligand concentration.

Changes in the ultraviolet absorption spectra at 330 nm at pH 2.9 were used to evaluate the equilibrium constant K_7' in solutions

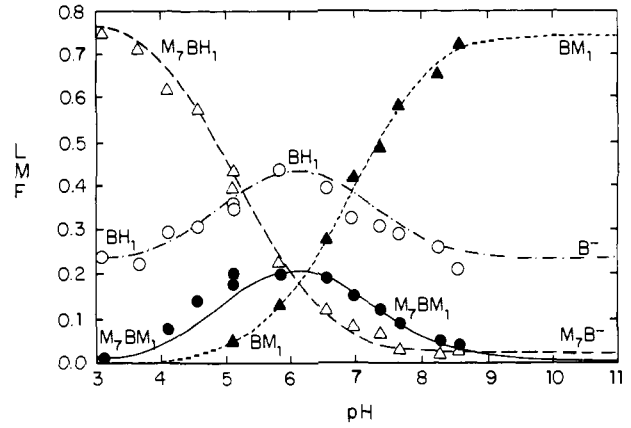

Figure 10. Species distribution of inosine binding by dienPd^{2+} presented as ligand mole fraction (LMF) vs. pH at 0.10 M dienPd^{2+} and 0.13 M total inosine. Curves derived from equilibrium constants in Table V correspond well to the experimental points. Symbols are the same as in the Figure 1 caption.

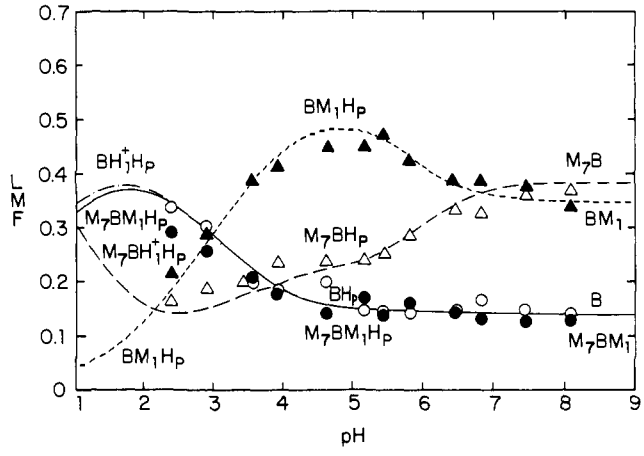

Figure 11. Species distribution of AMP binding by dienPd^{2+} presented as ligand mole fractions (LMF) vs. pH with both total dienPd^{2+} and total AMP at 0.1 M. Curves derived from equilibrium constants in Table V compare favorably with experimental points. Symbols are the same as in the Figure 1 caption.

containing 0.05 mM dienPd^{2+} and 0.05 to 0.25 mM inosine at natural ionic strength. Substitution of an O by an N donor to dienPd^{2+} produces a blue shift of the absorption band. From these H_2O solutions log $K_7' = 5.17 \pm 0.04$, a figure which agrees well with the NMR result of 5.34 ± 0.1 obtained in D_2O solutions at much higher ionic strength.

For inosine the N(1) proton has been removed from the B^-, M_7B^-, BM_1, and M_7BM_1 species while it is retained on the BH_1 and M_7BH_1 species. Thus it is possible to anticipate the results of a potentiometric titration curve by using the constants of Table V to calculate the fraction of deprotonated ligand. For a solution 3.0 mM in inosine and 1.5 mM in dienPd^{2+}, the calculated titration curve from pH 4.5–8.5 agreed with the observed curve to within 0.07 log units. To obtain a stable pH in the titration, long delays of up to 30 min were necessary after each addition of hydroxide ion. The rearrangement of dienPd^{2+} from N(7) in acid solutions to N(1) as the pH is increased is slow. For NMR experiments the pH was always checked before and after each measurement to guarantee that equilibrium had been reached.

Figure 11 shows a distribution curve for equimolar 0.1 M solutions of AMP and dienPd^{2+}. The concentration of the M_7B and BM_1 complexes in neutral solutions are comparable. The scheme in Figure 7 requires modification for AMP; phosphate protonation occurs at higher pH than base protonation to give the species BH_P and M_7BH_P instead of BH_1 and M_7BH_1. In addition the phosphate protonated species BM_1H_P appears, described by the constants K_1' and K_{a1P}. A distribution curve for 0.10 M adenosine is not presented as a figure because at pH >5

the molar ratio of BM_1 to M_7B is 4 and the curve becomes relatively nondescript with the BM_1 mole fraction of 0.65 the only species present in greater than 0.15 mole fraction.

Discussion

Chemical Shifts. All protonations on the nucleic bases produce the expected downfield chemical shift of the H(5) and H(6) protons in the pyrimidines and the H(2) and H(8) protons in the purines. Extraordinary are the H(8) downfield shifts of 0.98 ppm in GMP (Table I) and 0.88 ppm in IMP (Table II) upon N(7) protonation of BH_1H_P to give $^+H_7BH_1H_P$. In contrast, a H(2) downfield shift of only 0.06 ppm occurs in IMP upon protonation of B^- at nearby N(1) to give BH_1, while the more distant H(8) undergoes a 0.15 ppm downfield shift. In GMP and IMP metalation of BH_1H_P at N(7) to give $M_7BH_1H_P$ produces downfield shifts of both H(8) and H(2) protons that are 37–45% of the protonation shifts. This percentage compares with values of about 35% for Pd^{2+} binding/protonation found in ^{13}C NMR shifts[3] and for changes in bond lengths and bond angles in pyrimidines.[15]

In contrast to the above "normal" fractional changes of metalation/protonation are the chemical shifts produced by $dienPd^{2+}$ binding and protonation of N(1). In adenosine $dienPd^{2+}$ binding at N(1) to give BM_1 yields an upfield H(2) shift of 0.39 ppm which is 0.17 ppm greater than that produced by protonation to give BH_1^+. In IMP H(2) of BM_1 appears 0.05 ppm upfield from B^-, opposite to the normal direction. Somewhat more regularity develops with comparisons among species metalated at N(7). Nevertheless by the chemical shift comparison criterion more profound electronic rearrangements occur upon binding to N(1) than to N(7).

Figures 1, 3, and 5 show exceptions to the general observation that deprotonation induces upfield chemical shifts in a molecule. Deprotonation of the phosphate group of GMP, IMP, and AMP produces marked H(8) downfield shifts of 0.10–0.14 ppm in the free ligand and greater values of 0.25–0.27 ppm in both mononuclear and binuclear complexes that bear a $dienPd^{2+}$ at N(7). The magnitude of these shifts compares to the upfield shifts produced upon protonation at N(1), directly on the purine ring. As a result the chemical shift titration curves for the BH_1H_P and $M_7BH_1H_P$ species of GMP and IMP in Figures 1 and 3 display a bell shape. Corresponding curves for AMP in Figure 5 exhibit an inverted bell shape as the order of phosphate and N(1) deprotonations is reversed. Upon phosphate deprotonation the H(8) downfield shift of the AMP BM_1H_P complex is 0.10 ppm, comparable to that in the free ligand. Due to the absence of significant concentrations of the BM_1H_P complex in GMP and IMP, the extent of the H(8) phosphate deprotonation shift remains unknown, but it also occurs downfield. Thus the free ligand and three complex species yield downfield H(8) shifts upon phosphate deprotonation. Except for a small downfield shift of 0.025 ppm in unbound AMP, all corresponding H(2) phosphate deprotonation shifts are upfield. The explanation for the H(8) downfield phosphate deprotonation shifts in 5′-mononucleotides is uncertain, but they have been ascribed to the anti conformation.[16] Whatever the explanation, it must account for the two times greater H(8) downfield shift when $dienPd^{2+}$ is coordinated at N(7).

Protonation and Stability Constants. Upon comparing the stability constant for $dienPd^{2+}$ complexation at N(1) in purines and N(3) in pyrimidines with the pK_a for protonation at this site a close correlation appears. Combination on a single plot of log K_1 vs. pK_{aB} and log K_{71} vs. pK_{a7B} for the five purine ligands of Table V and log K_3 vs. pK_a for the three pyrimidine ligands of Table IV yields a straight line of slope 0.63 ± 0.03 for 13 points. Thus, whether or not the purines are metalated at N(7), there is a strong correlation between the stability constant logarithm and pK_a for binding at N(1).

Coordination of $dienPd^{2+}$ at N(7) of purine bases acidifies the proton at N(1). The difference between pK_{aB} and pK_{a7B} for the five ligands in Table V ranges from 1.1 to 1.9 log units with adenosine > AMP > inosine > IMP > GMP. This difference is about 0.18 log units greater for adenosine and inosine than for their 5′-monophosphates. For inosine the difference of 1.46 log units is somewhat less than the value of 2.1 found for the $(NH_3)_5Ru^{III}$ complex.[17] A similar difference of 1.9 log units has been reported for guanosine and $(NH_3)_5Ru^{III}$.[18] For H^+ the difference is about 2.1 log units for guanosine (see below). Thus metalation of purines at N(7) acidifies the N(1) proton by up to the 2.1 log units that is produced by protonation at N(7).

Table VI. Intrinsic Log [N(1)]/[N(7)] Binding Ratios

	H^+	CH_3Hg^+	$dienPd^{2+}$
inosine	5.7	4.5[a]	1.5
5′-IMP	5.2		0.8
guanosine	5.1	3.6[a]	
5′-GMP	4.6		−0.2
adenosine	3.0		0.6
5′-AMP	2.7		−0.1 (0.4)[b]

[a] Reference 19. [b] Phosphate protonated complex.

The basicity of the N(1) nitrogen plays a large role in determining the ligand distribution (Figures 8–11). Bound at N(7) in the most acidic solutions, $dienPd^{2+}$ competes more successfully with the proton for the N(1) site as the acidity drops. Not only the mole fraction of BM_1 becomes larger, but also that of M_7BM_1, which reaches a maximum near the point where the M_7BH_1 and BM_1 mole fractions are equal. In solutions without any free $dienPd^{2+}$, an increase in the mole fraction of the binuclear M_7BM_1 complex demands the same increase of free ligand. This dual increase is most evident in Figures 9 and 10 for IMP and inosine in the pH 5–9 region. Ligand distributions for IMP and inosine are similar with that for inosine displaced to lower pH by 1.2 units. The crossover pH, where M_7BH_1 and BM_1 appear in equal amounts, is strongly influenced by pK_{aB} for deprotonation at N(1). The crossover pH occurs at pH 1.4 for adenosine, 2.2 for AMP, 6.1 for inosine, and 7.3 for IMP. Though the GMP N(1) site is only 0.6 log units more basic than that of IMP, no crossover occurs for GMP in Figure 8. This result indicates that additional factors such as the relative binding strengths for metal ion at N(1) and N(7) influence the ligand distribution.

The last column of Table VI shows the value of log (K_1/K_7) from the constants tabulated in Table V. Addition of a 5′-phosphate to either inosine or adenosine decreases the value by about 0.7 log units, most of which may be attributed to the electrostatic effect of the dianionic phosphate favoring metalation at N(7) over N(1). The only other metal ion for which log (K_1/K_7) has been determined appears to be CH_3Hg^+, and its values[19] are also listed in Table VI.

N(1)/N(7) Mole Ratios. The intrinsic tendency of a proton to bind at N(1) or N(7) may be estimated by consideration of a microconstant scheme analogous to the K_1 and K_7 pathways for metalation shown in the right-hand cycle of Figure 7. From the observed titration constants for guanosine, $pK_1 = 9.2$ and $pK_{17} = 2.0$.[2] The two microconstants in the other limb of the cycle leading to the cation $^+H_7BH_1$ may be estimated by utilizing 7-methylguanosine as a model for $pK_{71} = 7.1$.[20] The properties of a cyclic system yield $pK_7 = 9.2 + 2.0 - 7.1 = 4.1$. The ratio log (K_1/K_7) is then 5.1, which value appears in the column labeled H^+ in Table VI under the entry for guanosine. The difference $pK_1 - pK_{71} = 2.1$ found for guanosine is applied to other purine rings, and in the case of nucleotides a small allowance is made for a charged phosphate group, to give the other values in the H^+ column in Table VI. In addition, we have utilized an estimated $pK_{17} = -1.6$ from ultraviolet spectra for protonation at N(7) of adenosine.[21] The H^+ column in Table VI provides the first

(15) Sinn, E.; Flynn, C. M., Jr.; Martin, R. B. *Inorg. Chem.* **1977**, *16*, 2403.
(16) Schweizer, M. P.; Broom, A. D.; Ts'O, P. O. P.; Hollis, D. P. *J. Am. Chem. Soc.* **1968**, *90*, 1042.
(17) Clarke, M. J. *Inorg. Chem.* **1977**, *16*, 738.
(18) Clarke, M. J.; Taube, H. *J. Am. Chem. Soc.* **1974**, *96*, 5413.
(19) Simpson, R. B. *J. Am. Chem. Soc.* **1964**, *86*, 2059.
(20) Lawley, P. D.; Brookes, P. *Biochem. J.* **1963**, *89*, 127.
(21) Mariam, Y. H.; Martin, R. B., unpublished research performed in **1978**.

extensive listing of intrinsic proton binding tendencies at N(1) and N(7) of purines. The N(1)/N(7) intrinsic binding ratio for protons is 2 log units greater for the 6-oxopurines than for adenosine.

The N(1) to N(7) dienPd^{2+} binding ratios in the last column of Table VI have ramifications for the ligand distribution curves. The relatively pronounced favoring of N(1) for IMP and inosine in Figures 9 and 10 results in BM_1 clearly predominating over M_7B^- in basic solutions. In contrast the negative logarithm for GMP in Table VI means that the mole fraction of M_7B^- exceeds that for BM_1 and no crossover occurs; the N(7) metalated complex predominates at all pH values. Basic solutions of GMP and dienPd^{2+} contain a mixture of four species, all present in significant amounts.

The intrinsic N(1)/N(7) binding ratios of Table VI show quantitatively that the tendency to favor N(1) over N(7) is $H^+ > CH_3Hg^+ >$ Pd(II). Indeed for dienPd^{2+}, the binding constant at N(7) is often comparable to or even exceeds that at N(1). For inosine the crossover pH, where the M_7BH_1 and BM_1 mole fractions are equal, occurs at pH 6.1 with dienPd^{2+}, 1.8 log units higher than with CH_3Hg^+, which is due to the lesser N(1)/N(7) binding ratio for dienPd^{2+}.

For AMP the values of log (K_1/K_7) and log (K_1'/K_7') are −0.1 and 0.4, respectively, the primes referring to phosphate protonated species. Compared to the monoanionic phosphate, the dianionic phosphate group favors dienPd^{2+} binding at N(7) over N(1). Thus there are two crossovers between N(7) and N(1) metalated species for AMP in Figure 11. The first crossover appears at pH 2.2 as $M_7BH_1H_P$ gives way to BM_1H_P when dienPd^{2+} successfully competes with H^+ for N(1). The maximum role fraction of BM_1H_P occurs near pH 5. Phosphate deprotonation near pH 6 yields a crossover close to pH 7, above which M_7B predominates marginally over BM_1 according to the −0.1 entry in the last column of Table VI.

We now compare the order of nucleotide binding strengths of dienPd^{2+} with the proton and CH_3Hg^+, the only other metal for which a series of reliable values exists. As previously, we designate the nucleoside by its capitalized first letter and the nitrogen binding site by the usual numbering scheme.[2] The order of decreasing proton binding strengths is then T3 > U3 > G1 > I1 ≫ C3 > A1 > G7 > I7 > A7. The order of CH_3Hg^+ is similar, with a promotion of G7 and I7 to greater than A1. These two sites undergo further significant promotion in the series for decreasing dienPd^{2+} stability constants T3 > U3 > I1 > G7 > G1 > I7 ≫ C3 > A1 > A7 with A1 and A7 now of comparable magnitude. Because of the proton at N(1) in purines and N(3) in pyrimdines the stability order, as opposed to stability constants, is pH dependent. At pH 7 the stability order for dienPd^{2+} becomes G7 > I7 > I1 > G1 > U3 > T3 > C3 > A1 > A7. This order agrees with that observed in neutral solutions of nucleotide mixtures.[7] Thus N(7) of GMP and IMP offers the strongest effective nucleic base binding site for dienPd^{2+} in neutral solutions.

The Effects of Methyl Group Substitution on Metal-Coordinated Cyclopentadienyl Rings. The Core and Valence Ionizations of Methylated Tricarbonyl(η^5-cyclopentadienyl)metal Complexes

David C. Calabro, John L. Hubbard, Charles H. Blevins II, Andrew C. Campbell, and Dennis L. Lichtenberger*

Contribution from the Department of Chemistry, University of Arizona, Tucson, Arizona 85721.
Received February 23, 1981. Revised Manuscript Received June 22, 1981

Abstract: Gas-phase He I, He II, and Mg Kα photoelectron spectra are reported for molecules of the type $(\eta^5\text{-}C_5H_{5-n}(CH_3)_n)M(CO)_3$ where $n = 0, 1, 5$ and M = Mn, Re. The influence of methyl groups on the cyclopentadienyl ring is monitored by shifts in both core and valence ionization energies. This enables effective separation of electron density transfer (inductive) and ring-methyl orbital overlap (hyperconjugative) effects. While the shift in the ring e_1'' ionization is found to be primarily a hyperconjugative effect, the shift in the metal valence ionizations is caused essentially entirely by a shift of electron density toward the metal atom. A greater proportion of this increased density is transferred to the carbonyls in the rhenium complexes than in the manganese complexes, indicating the greater back-bonding ability of the third-row atom. Further evidence of extensive Re–CO back-bonding is provided by the presence of vibrational fine structure on one of the predominantly metal ionizations of the rhenium complexes. This structure is the vibrational progression of the symmetric metal–carbon(CO) stretching mode. The long vibrational progression observed in this band and the frequency of the M–C stretch in the positive ion are direct evidence of considerable π back-bonding from the metal to the carbonyls. The observed vibrational structure in the spin–orbit split rhenium d ionizations also leads to a definitive interpretation of the pattern of metal ionizations in such complexes. The origin of the characteristic splitting of the predominantly ring e_1'' ionization is also considered in detail. The data suggest that the carbon–carbon bond distances in the ring are distorted an average of 0.01 to 0.02 Å from fivefold symmetry when coordinated to a d^6 ML_3 species. This is the first indication from gas-phase spectroscopy for such distortions.

The cyclopentadienyl ring ligand has played an important role in the development of organometallic chemistry since the discovery of ferrocene in 1952. The significance of the cyclopentadienyl ligand has stimulated interest in investigating the chemistry of other closely related ligands, such as rings in which one or more of the hydrogen atoms are substituted by other groups.[1] The most useful developments in this direction have been the synthesis of pentamethylcyclopentadienyl complexes, many of which are analogous to the well-known sandwich and half-sandwich compounds. Although at first glance the permethylation of cyclopentadienyl rings might appear to be a relatively minor alteration, it has proven to be a useful perturbation for mechanistic studies and has uncovered a significantly different chemistry in many systems.[1-3] For instance, the permethylated analogues have

(1) (a) King, R. B. *Coord. Chem. Rev.* **1976**, *20*, 155. (b) Fagan, P. J.; Manriquez, M. J.; Marks, T. J. In "Organometallics of f Elements"; D. Reidel: Dordrecht, 1979; p 113.

(2) (a) Bercaw, J. E.; Marvich, R. H.; Bell, L. G.; Brintzinger, H. H. *J. Am. Chem. Soc.* **1972**, *94*, 1219. (b) Bercaw, J. E. *Ibid.* **1974**, *96*, 5087.

0002-7863/81/1503-6839$01.25/0